FOWLER, JOSHUA, M.S. Roles of Endothelial Dysfunction and Injury in Mercury-induced Cardiotoxicity. (2019)
Directed by Dr. Zhenquan Jia 41 pp.

Cardiovascular disease (CVD) is the leading global cause of mortality and morbidity and presents a significant economic impact in the form of healthcare costs. The development of cardiovascular disease has many facets ranging from unhealthy lifestyle choices to unavoidable environmental toxins. Among these toxins that contribute to CVD, environmental and dietary exposure to organic mercury, in the form of methyl mercury (MeHg), presents a considerable cause for concern. Human exposure to this toxin has increased as a surge of industrialization sweeps the globe and many people are unaware that their normal diet, especially intake of fish and rice, has exposed them to MeHg. While traditionally labeled a neurotoxin, MeHg has been epidemiologically linked to CVD pathologies; However, its role in development and promotion of atherosclerosis, an initial step in more immediately life-threatening CVDs, remains unclear. Human microvascular endothelial cells (HMEC-1) are a well-characterized endothelial cell line that retains many important biomarkers and properties of human vascular cells. This study was conducted to examine the role that MeHg plays in the adhesion of circulating monocytes to vascular endothelial cells, a critical step in atherosclerosis, and attempts to clarify the underlying mechanisms. MeHg treatment significantly induced the adhesion of monocyte to HMEC-1 endothelial cells, while also upregulating the production of proinflammatory cytokines interleukin-6 (IL-6), interleukin-8 (IL-8). Further, MeHg treatment also upregulated the chemotactic cytokine monocyte chemoattractant protein-1 and intercellular adhesion molecule-1 (ICAM-1).

These molecules are imperative for the firm adhesion of leukocytes to endothelial cells. Additionally, the nuclear factor kappa B (NF-κB) signaling pathway is an important regulator in the expression of adhesion molecules and chemokines. Our results further demonstrated that MeHg stimulated a significant increase in NF-κB activation as measured by the eLUCIdate™ NF-κB reporter cell line. These findings suggest that NF-κB signaling pathway activation by MeHg is an important factor in the binding of monocytes to endothelial cells. Finally, cell death by necrosis has been suggested to contribute to endothelial cell dysfunction promoting cytokine release into the surrounding cellular matrix, exacerbating atherosclerotic development [1]. By using flow cytometric analysis with 7-AAD and AnnexinV/PI, MeHg treatment only caused a significant increase in necrotic cell death at 2.0 μM concentrations without initiating apoptosis. This study provides new insights into the molecular actions of MeHg that can lead to endothelial dysfunction, inflammation and subsequent atherosclerotic development. This contributes to our understanding of the detrimental effects of human exposure to MeHg which remains an important human health concern in a rapidly industrializing world.

ROLES OF ENDOTHELIAL DYSFUNCTION AND INJURY IN MERCURY-INDUCED CARDIOTOXICITY

by

Joshua Fowler

A Thesis Submitted to
the Faculty of The Graduate School at
The University of North Carolina at Greensboro
in Partial Fulfillment
of the Requirements for the Degree
Master of Science

Greensboro
2019

Approved by

_____
Committee Chair

APPROVAL PAGE

This thesis written by Joshua Fowler has been approved by the following committee of the Faculty of The Graduate School at The University of North Carolina at Greensboro.

Committee Chair _____
Zhenquan Jia

Committee Members_____
Ramji Bhandari

_____
Dennis LaJeunesse

_____
Martin Tsz-ki Tsui

_____
Date of Acceptance by Committee

_____
Date of Final Oral Examination

TABLE OF CONTENTS

Page

LIST OF FIGURES iv

CHAPTER

I. INTRODUCTION 1

II. MATERIALS AND METHODS 11

III. RESULTS 18

IV. DISCUSSION 27

REFERENCES 37

LIST OF FIGURES

Page

Figure 1. Monocyte Adhesion to HMEC-1 Cells Following MeHg Treatment 19

Figure 2. Gene Expression of Cytokines in HMEC-1 Cells Following MeHg Exposure 20

Figure 3. NF-kB Reporter Cell Line Response to MeHg Treatment 21

Figure 4. Phase II Antioxidant Gene Expression in HMEC-1 Cells After MeHg Treatment 23

Figure 5. Phase II Antioxidant Levels in EaHy926 Cells After MeHg Treatment 23

Figure 6. Flow Cytometry Results for HMEC-1 Cells Following MeHg Treatment 25

Figure 7. Representative Flow Cytometry Results in HMEC-1 Cells Following MeHg Treatment 26

CHAPTER I

INTRODUCTION

Atherosclerosis and the Development of Plaque

Atherosclerosis develops due to an inflammatory pathway activated by many potential xenobiotics. Initially, the endothelial cellular membrane lining the walls of arteries experiences damage from Oxidized low-density lipoprotein (Ox-LDL) which is present in the subendothelial space. This is due to different environmental or dietary factors that cause oxidative damage. Ox-LDL then promotes the expression of adhesion molecules, like ICAM-1 and VCAM-1, which migrate to the cell surface and participate in the capture and migration of circulating monocytes [2]. These adhesion molecules are further stimulated by other cytokines like IL-1β and TNF-α, a powerful inducer of the NF-kB pathway [3]. Monocytes naturally express complementary cell-surface β_2-integrins, like MAC-1 and LFA-1, and VLA-4 which stabilize this adhesion process by binding to ICAM-1 and VCAM-1, respectively [2, 4]. This cell-surface binding and adhesion allows for the migration of monocytes into the intima of a blood vessel.

Migration of monocytes can be aided by chemotactic cytokines like MCP-1 (CCL2) and CCL5. These chemotactic molecules promote the movement of monocytes through the endothelial layer and allow them to deposit in the vessel. Once deposited, these monocytes differentiate to macrophages and begin expressing scavenger receptor such as CD36 and CD68 [5]. Scavenger receptors aid in the phagocytotic action of

macrophages. However, ingestion of Ox-LDL causes the cell to become laden with lipid molecules and develop into a foam cell. These cells can then lyse and release proteases into the subendothelial space, weakening the protective fibrous cap of the vessel. Continued failure to clear apoptotic cells, increased recruitment of monocytes, and subsequent lysis of macrophages creates a positive feedback cycle that can lead to thrombosis of the vessel.

Further promoting this feedback loop, the production of pro-inflammatory cytokines due to endothelial injury encourages further recruitment of monocytes to the subendothelial space. Ox-LDL can promote the production of TNF-α, which acts as a stimulator of the canonical NF-kB pathway. Under normal conditions, canonical NF-kB exists in the cytosol as p50 and RelA subunits and is heavily regulated by a third bound IkB molecule. After stimulation of the tumor necrotic factor receptor (TNFR) by TNF-α, the receptor recruits an IKK complex, which contains subunits capable of phosphorylating the regulatory IkB subunit, tagging it for degradation. Once degraded, the remaining p50 and RelA subunits are able to translocate into the nucleus of a cell facilitating the upregulation of adhesion molecules, like VCAM-1 and ICAM-1, and also other chemotactic and inflammatory chemokines such as IL-8, IL-6, CXCL1, CXCL2 and CXCL3 [6] Evidence also links these molecules as potentially aiding in the trapping of monocytes [2].

ROS Implications in Atherosclerosis

Atherosclerosis and subsequent CVD pathologies are multifaceted. however, the overproduction of Reactive Oxygen Species (ROS) has been shown to be an initiating factor. ROS exist in many forms, hydroxyl radicals (OH•), superoxide anions (O2-•), peroxides (H_2O_2), and peroxynitrites (ONOO), and are critical for normal cellular functions. For example, Peroxides can cross cellular membranes and so promote cellular signaling [7]. However, an overproduction of ROS has been implicated in disruption in major cellular components such as antioxidant proteins, lipid bilayers, and DNA, thus leading to the endothelial dysfunction, and development of atherosclerotic plaques [8].

ROS are named as such due to their reactivity to neighboring molecules. Perhaps most importantly, ROS are able to oxidize nearby low-density lipoproteins into Ox-LDL, initiating endothelial damage and promoting the activity of cellular adhesion molecules. Further, studies have shown that Ox-LDL can promote the production of intracellular ROS. In a study conducted on bovine aortic endothelial cells (BAEC), administration of Ox-LDL increased intracellular ROS production in a dose-dependent manner through the lectin-like receptor, LOX-1 [9]. Activation of this receptor also triggers the NF-kB pathway, which promotes the production of adhesion molecules and inflammatory chemokines [10]. Additionally, the increased presence of intracellular ROS can lead to lipid peroxidation of the cellular membrane, disruption of antioxidant or protein redox balance, and mitochondrial function.

Mitochondrial dysfunction is the first step in the overproduction of ROS. As cardiovascular cells have a high level of metabolic activity, the mitochondria in these

cells are of particular importance. The electron transport chain (ETC) utilizes oxidative phosphorylation to produce ATP for the cell, and in the process, can generate ROS as an intermediate, or through "electron leakage" [11]. Donation of a single electron to O_2, yields a superoxide radial ($O_2^{\cdot -}$) and a second electron yields peroxide, H_2O_2. A third electron can be donated through a Fenton reaction to yield a hydroxyl radical (·OH) and finally a fourth yields water. Endothelial dysfunction and intracellular ROS can encourage the mitochondrial overproduction of ROS in a positive feedback mechanism. Complex I and Complex III of the ETC generate $O_2^{\cdot -}$ radicals and the mitochondrial enzyme manganese superoxide dismutase (SOD2) scavenges these superoxide radicals and converts them to peroxide. Damage to this enzyme by overproduction of ROS propagates the further overproduction of mitochondrial ROS, leading to endothelial dysfunction, apoptosis, and atherosclerosis. Additionally, the ROS produced by dysfunctional mitochondria can initiate multiple other detrimental effects in cells.

The outer layer of a cell is composed of an amphiphilic bilayer of lipids embedded with signaling proteins. Two main components of this lipid bilayer are arachidonic acid and linoleic acid. These lipids peroxidize into 4-hydroxynonenal (HNE) and malondialdehyde (MDA), which have been well-characterized as cytotoxic agents [12]. MDA, in particular, interacts with nucleic acids and can facilitate DNA damage in the cell [13]. Further, lipid radicals produced by reactions with ROS can, in turn, attack and damage neighboring lipids, creating a cascading effect of damage. In this process, the lipid bilayer of the cell is disrupted which can lead to endothelial dysfunction such as leakage of cellular contents and disruption of receptors embedded in the membrane [14].

As these cells are damaged in this way, they activate inflammatory and chemotactic pathways that contribute to the formation of atherosclerosis and progression of CVDs. However, lipids are not the only target of intracellular ROS.

Reactive oxygen species, in normal levels, can be used by cells to promote cellular signaling. This is done through redox cycling mediated by antioxidant molecules and phase II enzymes such as Glutathione (GSH) and its contributing enzymes: Glutathione S-transferase (GST), Glutathione peroxidase (GPx) and Glutathione reductase (GR). Glutathione becomes oxidized to GSSG by H_2O_2, with the aid of the enzyme GPx. It then can be reduced by NADPH with the enzyme GR, creating NADP+ in the process. GSH is typically found in the cell in higher concentrations than its oxidized counterpart, GSSG. However, the increase in ROS production shifts the balance to the oxidative state and decreased the ability of this redox cycle to regulate H_2O_2 [13] . As peroxide builds, the downstream effects of lipid peroxidation and DNA damage occur, triggering the upregulation of adhesion molecules, and inflammatory cytokines. This eventually leads to the furthering of atherosclerosis [11].

While its widely known that a sedentary lifestyle and poor dietary choices can lead to an increased incidence of CVD, a great deal of research is needed to identify potential environmental sources of toxins that promote ROS production, inflammation and consequently induce atherosclerosis. Epidemiological evidence exists that overwhelmingly supports the fact that industrial fumes contribute to declining in cardiovascular health, however, dissecting the detrimental agents in these fumes and their transformations in the immediate environment will allow us to better understand its

harmful effects to cardiovascular health. A major component of these industrial fumes is Mercury. Once mercury is put into the environment, a cascading effect occurs that has the potential to expose humans to the chemical. This exposure is possibly the initiating step in the aforementioned pathways leading to increased ROS and atherosclerosis.

Production of Methyl Mercury

Mercury primarily exists in three forms: inorganic, elemental, and organic. Inorganic mercury is found as salt and poses a risk to human health. Inorganic mercury is primarily found as industrial wastes and, in some cases, in small-scale artisanal gold mining [15]. Elemental mercury is mercury in its purest form, while not safe for humans, it is the most inert form. Organic mercury poses the most direct threat to human health due to its bioavailability. Organic mercury can exist as either methyl mercury, dimethyl mercury, or ethyl mercury. Ethyl mercury is found agriculturally as a fungicide and minimally in thimerosal-containing vaccines. Dimethyl mercury is an extremely potent neurotoxin and one of the most deadly chemicals known to humankind. However, methylmercury (MeHg) is the compound that presents the greatest immediate risk to human health due to its dietary and environmental prevalence and bioavailability.

While Mercury runoff from industry is primarily airborne and inorganic, it can fall to the earth through precipitation and collect in rivers, streams, and ponds. Bacteria are then able to ingest the mercury and through biomethylation, transform the toxin into methyl mercury [16]. We are then able to follow the food chain upwards as bacteria are ingested by plankton, which is ingested by fish, which are ingested by larger fish which

biomagnifies mercury concentration in the tissues of these animals. Indeed, as the mercury bioaccumulates in these organisms, they become a greater risk to human consumption. Tuna, Snapper, and other large, carnivorous fish are of particular risk as regular in the human diet, as they have bioaccumulated large concentrations of mercury [17].

Mercury as a Neurotoxin

Typically, mercury exposure has been linked to neurotoxicity and neurodegenerative disorders. Acute mercury toxicity and its links to neurodegeneration have been seen epidemiologically for many years. In the 1950's a great deal of industrial runoff entered the coastal waters of Japan and found its way into the food chain. Those people who's diet incorporated the infected fish and other wildlife of the surrounding waters began to exhibit ataxia, sensory disturbances, dysarthria, auditory disturbances, and involuntary tremors. This led to the discovery of MeHg as a neurotoxic agent [18]. While the mechanisms leading to MeHg neurotoxicity have not been completely defined, strong evidence suggests the overproduction of ROS as a culprit for the symptoms mentioned previously. [19]. Recent studies point to the fact that even low levels of MeHg exposure can cause a significant increase to ROS produced in the motor cortex of rats, leading to a decrease in motor skills. [20].

Further, the impact of MeHg exposure on developing fetuses has been extensively studied. Results show that MeHg ingested by a mother while pregnant can lead to behavioral abnormalities throughout a child's life, especially pertaining to language,

attention and memory [21]. This prolonged impact on behavior and neurological health drive a desire for greater understanding of neurotoxic pathways and impacts of ROS exposure. However, while a great deal of information exists on the neurotoxic impacts of MeHg, a literature gap exists that fails to explain the toxic effects of MeHg in other organ systems.

Mercury and Cardiotoxicity

While MeHg toxicity has been studied in various systems, the prevalence and impact of MeHg toxicity on the cardiovascular system is a new area of research. Epidemiological evidence from sites such as the Amazon rainforest, Finland, and the Faroe Islands have shown evidence that links diets high in MeHg to increased incidence or risk of cardiovascular disease [22-24]. In Finland, a study was done to link the dietary intake of high-MeHg fish to CVD in 1833 men between age 42 and 60 who had no previous incidence of CVD. Within the time frame of the study, 73 of the men experienced an acute myocardial infarction (AMI) within 2 to 7 years. 78 of the men died, of which 18 died of CHD and 24 from CVD. The study used hair mercury concentration and urinary mercury excretion, which correlated with fish intake. Final results indicated a 2.1-fold increase in the risk of AMI after attenuating the effect of other factors like family history and smoking habits [25].

In the Amazon rainforest, gold mining and hydroelectric damming of rivers release Hg into the environment, where it methylates and begins biomagnifying in fish. Nearby Amazonian tribes rely heavily on fish as a dietary source of protein and thus are

subjected to increased exposure to MeHg [26]. Studies by Grotto et al. 2010 included blood, hair, and plasma sampling from 108 individuals living along a major Amazonian tributary susceptible to environmental MeHg contamination. Analysis of catalase, GSH, GPx, and ALA-D biomarkers indicated a negative correlation between blood, hair and plasma MeHg concentrations and levels of oxidative stress biomarkers. This indicates a positive correlation between MeHg exposure and oxidative stress which can lead to CVD.

Studies in the Faroe Islands conducted by Sorensen et al. evaluated the effects of prenatal exposure to MeHg on blood pressure in childhood. The rationale was that early development of hypertension was a risk factor for the development of CVD. A sample size of 1022 single births was examined and cross-referenced with maternal hair mercury levels and umbilical cord blood mercury concentration. Children were reevaluated at age 7 for changes in blood pressure. Statistical analysis showed an average increase of 13.9 mmHg to the diastolic blood pressure and an average increase of 14.6 mmHg to systolic blood pressure.

With compelling epidemiological evidence, the next step in investigating the link between MeHg exposure and CVD would be to replicate MeHg exposure *in vitro* and *in vivo* as controlled animal studies. As discussed earlier, one of the driving forces behind atherosclerosis is the overproduction of ROS. Rat studies have indicated that even low levels of MeHg exposure can increase superoxide anion production [27]. This superoxide production, in turn, decreases the bioavailability of Nitric Oxide (NO), which is an important regulator of normal vasomotor tone in human coronary arteries [28]. Another

trial on Wistar rats showed that low-level MeHg exposure caused increased vascular $O_2^{\cdot -}$, elevated plasma MDA levels, and higher total antioxidant status, linking MeHg with atherosclerosis and increased ROS [29]. Mitochondrial studies on rats treated with inorganic mercury also showed the increased formation of H_2O_2, depletion of mitochondrial GSH, and 68% increased detection of peroxidized lipids [30]. This provides compelling evidence that MeHg may activate previously described atherosclerotic pathways leading to CVD.

As described above; MeHg, although typically considered a neurotoxin, has recently been implicated as a potential promoter of atherosclerosis in humans. However, its underlying mechanisms have not been discovered. As toxins can be transported through the body in blood, the effect of MeHg on endothelial cells is an important target to research. Recent studies have shown that endothelial dysfunction induced by inflammation promotes monocyte adhesion and migration to the subendothelial space, contributing to atherosclerosis [31-33]. We hypothesized that MeHg stimulates the adhesion of monocytes due to chemokines and adhesion molecules expressed. Human microendothelial cells (HMEC-1) are a well-characterized cell line that retains many important properties of endothelial cells. For example, they retain many of the chemotactic, adhesion molecules and inflammatory biomarkers found in other endothelial cell lines. This study took place to investigate the role and underlying molecular mechanisms of MeHg-induced endothelial dysfunction and damage. This work will provide a greater understanding of the cellular and molecular effects of MeHg exposure on vascular dysfunction to further determine cardiovascular risks of human exposure.

CHAPTER II

MATERIALS AND METHODS

Cell Culture

EA.hy926 (ATCC® CRL-2922™)– Cells were cultured in 8mL of Gibco glucose-rich Dulbecco's Modified Eagle Media (DMEM) supplemented with 10% Fetal Bovine Serum (FBS) and 1% Penicillin/Streptomycin. HMEC1 (ATCC ® CRL-3243™Cells were grown in GenDepot® MCDB 131 media, supplemented with 10mM L-glutamine, 10ng/mL Endothelial Growth Factor (EGF), 1µg/mL hydrocortisone and 10% FBS. THP-1 cells were grown in RPMI media supplemented with 10% FBS and 1% Penicillin/Streptomycin. eLUCIdate ™ RAW Nf-kB reporter cells were cultured in DMEM supplemented with 5% glutamate and 1% Penicillin/Streptomycin. Cell lines were grown in Cellstar® Filtered Cap 75 cm^2 cell-culture treated, screw cap flasks in incubators set to 37 degrees Celsius and 5% CO2. Media was renewed every 2-3 days and cells were split into a new passage at 85-95% confluence.

Cell Treatment

Cells were treated using a mixture of Sigma-Aldrich/Millipore Sigma® Hanks Balanced Salt Solution (HBSS) containing calcium, magnesium, glucose and Methyl Mercury in dose-dependent concentrations of 0.1 µM, 1.0 µM, and 2.0 µM for varying time intervals. Cells were split into 100mm x 10mm Corning® Cell culture plates and

allowed to grow to 85% confluence. Plates were then decanted of their media and rinsed 2 times with 1X PBS. 6mL of treatment was pipetted onto the adherent cells and plates were returned to the incubator at 37°C and 5% CO^2.

Antioxidant Enzyme Lysate

Cells were treated with MeHg using the methods described above. After 24 hours of incubation, cells were rinsed with PBS two times to remove any remaining media. 3mL of trypsin was then added per 75 cm^2 of growth surface area. Cells were then incubated for 4 minutes, and trypsin was neutralized with the addition of 6mL of FBS-containing growth media. This cell suspension was centrifuged for 10 minutes at 1,000 RPM to create a cell pellet. The cell pellet was then resuspended in 1mL of PBS, transferred to an Eppendorf tube and centrifuged again at 5,000 RPM for 5 minutes to rinse any remaining media. The resulting pellet was resuspended in 300 µL of Tissue Buffer containing KH2PO4/K2HPO4 with 2mM EDTA. The mixture was sonicated 4 times at 15-second intervals. The resulting solution was centrifuged at 13,000 RPM for 5 minutes and the supernatant collected and tested for antioxidant enzymes.

Monocyte Adhesion Assay

Cells were cultured to 85% confluence in their respective media, described above, and treated with varying concentrations of 0.1-2.0 µM Methyl Mercury for 4 hours. About 1.5 hours prior to the end of treatment, THP-1 monocytes were counted using a hemocytometer. Approximately 2.5 million cells per plate were then collected and

centrifuged at 1000 rpm for 7 minutes. The resulting cell pellet was resuspended in 10ml of RPMI media containing 0.5% FBS and 10% Pen/Strep. Next, 7.5µL of calcein was added to the THP-1 monocytes for labeling before allowing them 1 hour to incubate. Following incubation of treatment cells, the treatment media was decanted, and the cells washed with 1x phosphate buffered saline, twice. Labeled THP-1 monocytes were centrifuged at 1000 rpm for 7 minutes and then suspended in 6mL/plate of RPMI media as mentioned above. Then, cells were then incubated for 1 hour with calcein-labeled THP-monocytes. The cells were washed with cold 1x PBS, removing any unbound monocytes, then remaining cells were removed using a cell scraper and 1x PBS. The resulting mixture was transferred to a Costar® transparent 96-well plate and read at 496nm/520nm.

Protein Concentration Assay

Protein was measured using 10µL of lysate diluted in 790µL of DI H20. 200uL of Bio-Rad® Protein Assay Dye Reagent was then be added. The mixture will be vortexed and transferred to Cuvettes. Absorbance will be measured using the Beckman-Coulter® DU800 spectrophotometer at 595 nm with 1.48 mg/dL Bovine Serum Albumin as a standard.

Glutathione (GSH) Assay

EAhy926 and HMEC1 cells were grown to 90% confluence in treated cell culture plates and exposed to MeHg and HgCl concentrations mentioned above at varying time

intervals. An antioxidant enzyme lysate was produced, and 10µL of the lysate was then mixed with GSH buffer and HPO_3. This solution was centrifuged at 13,000 RPM for 5 minutes. The solution was then combined with GSH buffer in a separate Eppendorf tube and incubated with 100µL of O-phthalaldehyde (OPT) for 15 minutes in a dark room. 250µL of the resulting solution was pipetted to a black Costar® 96-well plate, and the absorbance was measured by excitation at 250nm and emission at 420nm. A blank of GSH buffer and a positive sample containing 100µL of GSH standard was also measured in the plate. The GSH content of samples was quantified using a standard curve previously created by our lab.

NAD(P)H Quinone Dehydrogenase 1 (NQO1) Assay

EAhy926/HMEC1 cells were grown to confluence, treated, and an antioxidant enzyme lysate was created using methods, described previously. A reaction master mixture was created using 15mL of Tris-HCl/NQO1 buffer, 45µL of 50mM Nicotinamide Adenine Dinucleotide Phosphate (NADPH) and 60µL of Dichlorophenolindopehnol (DCPIP). 4µL of the collected antioxidant lysate was then combined with 696 µL of the created master mix in a cuvette, and absorbance measured using the Beckman-Coulter ® DU800 spectrophotometer at 600nm. The rate kinetics of DCPIP reduction elucidated NQO1 activity.

RNA Extraction

HMEC1 cells were cultured in their appropriate media in Corning® cell culture treated plates until 90% confluent. The media was then decanted, and the cells were treated with varying concentrations of MeHg and HgCl as described above for varying time frames. After completion of the treatment, cell plates were rinsed twice with 1X PBS to ensure any remaining treatment media does not remain. Cells were treated with 1mL of TRIzol® and pipetted into 1mL Eppendorf tubes. 200µL of Chloroform was added, the solution was agitated and then transferred to a centrifuge at 12,000 RCF for 15 minutes. The top aqueous phase was combined with 500 µL of isopropanol and mixed well before being centrifuged again at 12,000 RCF for 10 minutes. The resulting pellet was washed and centrifuged at 7,400 RCF for 5 minutes twice before resuspending the pellet in 10-15µL of DEPC.

cDNA Synthesis

Cells were cultured, treated, and RNA was extracted using the methods stated above. The resulting RNA was quantified using a Thermo Scientific ™ Nanodrop 2000 and diluted to a 500ng/µL concentration. 2µL of dilute RNA was then combined with 5µL of 5X Buffer, 1.25µL of ddNTP, 1.25µL of Random Primer, 0.625µL of MMLV-Reverse Transcriptase and 14.875µL of DEPC water. The 25µL solution was converted to cDNA using the Applied Biosystems ™ Veriti ™ 96-Well Thermal Cycler.

Quantitative Real-time Polymerase Chain Reaction (aRT-PCR)

Cells were cultured and treated, and RNA was extracted and converted to cDNA using the methods stated above. The resulting cDNA was probed for IL-8, IL1β, IL-6, and MCP-1 using GAPDH as a housekeeping gene. This was done by combining 1µL of cDNA with 10µL of Power SYBR ® Green PCR Master Mix, 2µL of 1:10 diluted cDNA, 2µL of 5µM Forward Primer, 2µL of 5µM Reverse Primer and 5µL of DEPC. The Applied Biosystems™ StepOnePlus™ Real-Time PCR system was run for 40 cycles. Each cycle encompassed a 95°C phase for 15 seconds, a 58°C phase for 1 minute and a 60°C phase for 15 seconds. In order to quantify gene expression, Comparative Threshold values were evaluated.

NF-kB Luciferase Assay

eLUCIdate™ RAW 264 NF-kB report cell line cells were grown using previously mentioned media in 6-well plates. Cells were treated with various concentrations of MeHg for 4 hours. Following treatment, cells were washed twice with 1ml of cold PBS to remove any excess media. Cells were then lysed with lysis buffer on a shaker table for ~20 minutes. Finally, 2µL of coelenterazine was added to catalyze the luminescent reaction. Luminescence was ready using the Synergy ™ 2 Multi-Mode Microplate reader.

7-AAD/Annexin V-PI Flow Cytometry

Cells were cultured and treated as described previously. Confluent cells were then gently washed 2 times with cold PBS to remove any remaining media. A cell scraper was

used to remove any remaining cells, and the subsequent cell suspension was transferred to a microcentrifuge tube and centrifuged at 7000 RPM for 5 minutes. The supernatant was discarded, and cells were resuspended in 1X annexin-binding buffer to a concentration of 2.0 x 10^5 cells/ 100µL. Following resuspension, 2.5 µL of FITC-AnnexinV and 1 µL of 7-AAD were added per 100µL of suspension. The solution was incubated for 15 minutes at room temperature before addition of 400µL of binding buffer. The analysis was done using the Guava EasyCyte Flow Cytometry system.

CHAPTER III

RESULTS

Monocyte Binding in HMEC-1 Endothelial Cells Increases in a Dose-dependent Manner in Response to Treatment with Methyl Mercury

The critical first step in the development of atherosclerosis is inflammation or dysfunction induced monocyte adhesion to endothelial cells [31-33]. We measured the degree of this adhesion caused by MeHg exposure by performing a monocyte adhesion assay. HMEC-1 cells were treated with 0.1, 1.0, and 2.0 μM MeHg in HBSS then subsequently treated with calcein-labeled THP-1 monocytes. Absorbance was then read at 570nm. As shown in Figure 1, at 2.0 μM and 1.0 μM HMEC-1 cells displayed a significant ($p<0.05$) ~3.4-fold and~1.7-fold increase in monocyte adhesion, respectively when compared with control cells cultured in HBSS media alone. 0.1 μM treatments showed no significant change in monocyte binding compared to control. TNF-α, a known promotor of monocyte binding, was used a positive control and displayed a significant ($p<0.05$) ~3.4-fold increase in monocyte adhesion (**Fig. 1**).

Figure 1. Monocyte Adhesion to HMEC-1Cells Following MeHg Treatment. HMEC-1 cells were treated with 0.1, 1.0, and 2.0 μM MeHg for 4 hours in Hanks' balanced salt solution (HBSS). Cells were then co-treated with calcein-labeled THP-1 monocytes and absorbance was read at 570nm via Biotech Synergy 2 plate reader. All data represent mean ± SEM. (n=4, *, P< 0.05 vs. control.)	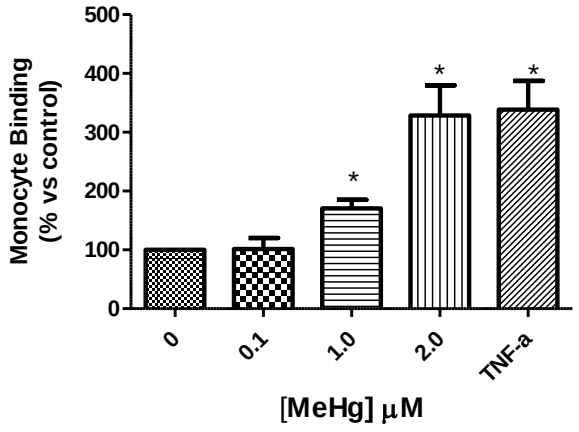

Levels of Inflammatory Cytokine Gene Expression in HMEC-1 Cells Following Methyl Mercury Exposure

Adhesion of monocytes to ECs is regulated by several critical chemotactic and inflammatory cytokines, as well as the presence of vascular adhesion molecules on the cell surface. Using qRT-PCR, we probed HMEC-1 cells treated with different concentrations of MeHg for changes in gene expression of these molecules. Levels of IL-8, IL-6, ICAM, and CCL2 in HMEC-1 cells treated for 4 hours with 0-2.0 μM MeHg were quantified using qRT-PCR. As shown in **Figure 2A**, IL-8 levels of gene expression increased significantly ($P < 0.05$) by 18-fold in 1.0 μM treatment group and appear near significantly ($P=0.06$) upregulated by 163-fold in 2.0 μM treatment group. Expression of IL-6 significantly ($P<0.05$) increased by 4-fold in 1.0 μM treatments and by 17.7 in 2.0 μM treatments (**Fig. 2B**). CCL2 levels significantly ($P<0.05$) increased in 2.0 μM

treatments by 63.7-fold (**Fig. 2C**). Finally, ICAM expression also significantly increased ($P<0.05$) by 14-fold in 2.0 μM treatments and near significant increase ($P=0.052$) of ~2-fold at 1.0 μM treatment (**Fig. 2D**).

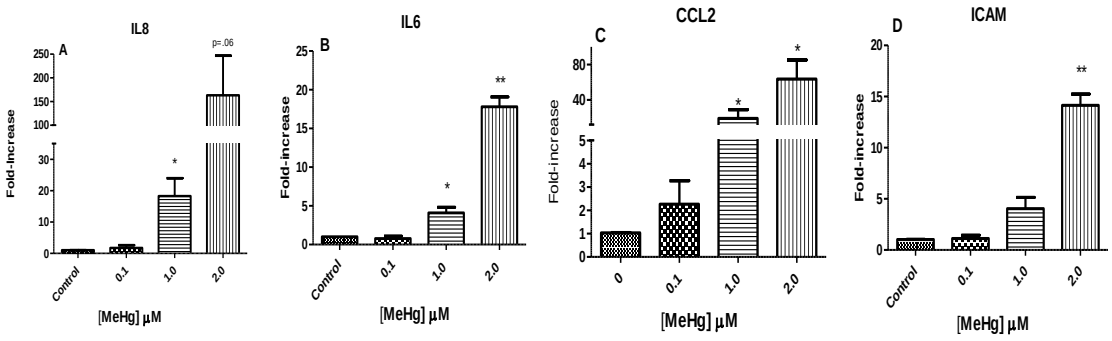

Figure 2. Gene Expression of Cytokines in HMEC-1 Cells Following MeHg Exposure. HMEC-1 cells were treated with 0.1, 1.0, and 2.0 μM MeHg for 4 hours in HBSS. RNA was isolated, converted to cDNA and probed for IL-8 (A), IL-6 (B), CCL2 (C), and ICAM (D) using SYBRgreen qRT-PCR reagents via QuantStudio 3. GAPDH was used as a housekeeping gene. All data represent mean ± SEM. (n=3, *, $p< 0.05$ vs. control. **, $p< .01$ vs. control)

Examination of Activation of the NF-kB Pathway due to Methyl Mercury Exposure

Studies show that NF-κB-mediated (Nuclear factor kappa B) transcription of the previously described cytokines and adhesion molecules plays an important role in atherosclerotic pathology [34-36]. Activation of this signaling pathway results in a greater magnitude of leukocyte adhesion to endothelial cells. We chose to examine whether MeHg exposure is implicated in the activation of this pathway by using the eLUCidate NF-κB reporter cell line. This cell line has been well characterized and has been widely used to detect changes in the NF-κB transduction pathway. These cells contain a Renilla luciferase reporter gene under direct transcriptional control of the

upstream NF-κB response element in DNA. By introducing coelenterazine as a substrate, we were able to induce luminescence in living cells. The intensity of this luminescence directly correlates with NF-κB pathway activation. As shown in Figure 3, cells treated with 2.0 μM MeHg for 4 hours showed a significant ($P<0.05$) increase by 4.5-fold in luminescence. This finding indicates that MeHg promotes the binding of NF-κB transcription factors to response elements on DNA, inducing the transcription of the luciferase reporter gene, as well as a potential transcription of any downstream cytokines. Lipopolysaccharide, a known activator of the NF-kB pathway, was used as a positive control and induced a significant ($P<0.05$) 8.6-fold increase in luminescence (**Fig. 3**).

Figure 3. NF-kB Reporter Cell Line Response to MeHg Treatment. NF-kB RAW cells were treated with 0.1, 1.0, and 2.0 μM of MeHg in HBSS for 4 hours. Coelenterazine was then added as a substrate at a concentration of 1 μM, and luminescence was read using the Biotech Synergy 2 plate reader. LPS at 10μg/ml was used as a positive control. All data represent mean ± SEM (n=3. *, $p<0.05$).

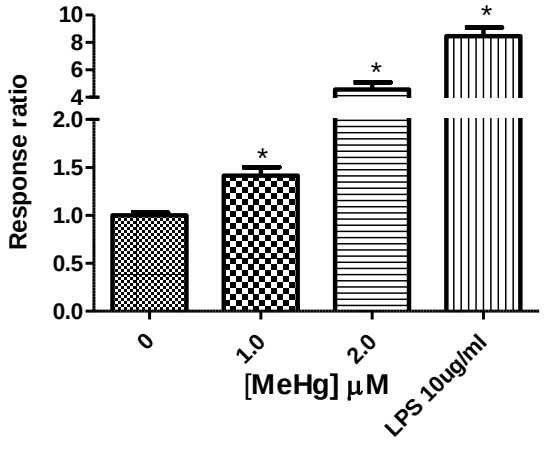

Phase II Antioxidant Levels Show No Significant Changes in Response to Methyl Mercury Treatments

Studies have implicated phase II cellular antioxidant enzymes, such as glutathione (GSH) and NAD(P) H dehydrogenase (quinone)-1 (NQO-1) as important drivers of ROS-mediated adhesion molecule expression in endothelial cells [5]. Both GSH and NQO1

are important cellular antioxidants in the cells that protect them against oxidative damage from reactive oxygen species (ROS). qRT-PCR was performed to measure the relative gene expression of gamma-glutamyl cysteine ligase (GCL) and NQO1 in cells treated for 4 hours with 0 – 2.0 μM. GCLc is an important precursor molecule involves in the synthesis of GSH. Treatment showed no significant ($P < 0.05$) changes in the gene expression of GCLc (**Fig. 4a**), or NQO1 (**Fig. 4b**) in HMEC-1 cells. To further validate these findings, we employed EAhy926 cells, an additional human endothelial cell line. EAhy926 cells cultured for 24h with 0.1, 1.0, and 2.0 μM MeHg in HBSS were measured for total protein levels as a standard before quantifying changes in antioxidant enzymes. As shown in Figure 5, the levels of GSH and NQO1 (nmol/mg protein) showed no significant changes ($P <0.05$) in response to any methyl mercury treatment concentrations.

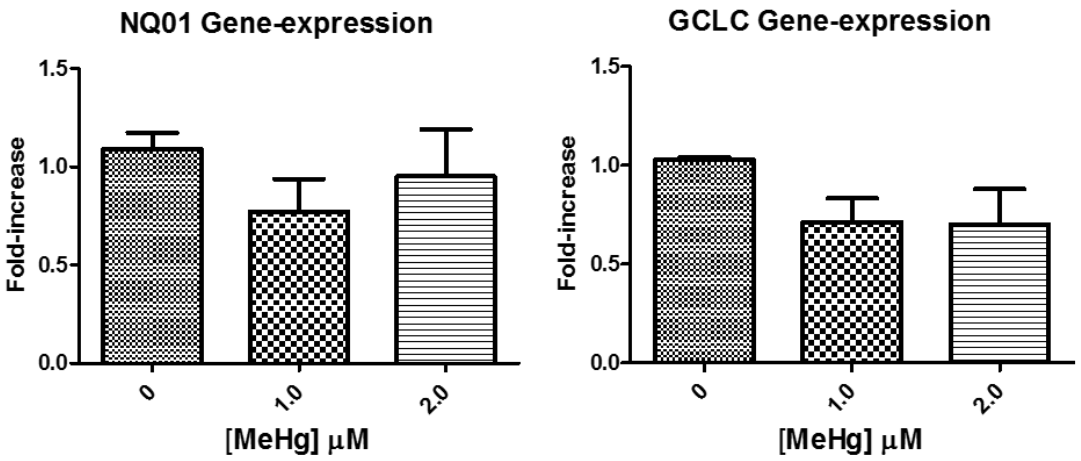

Figure 4. Phase II Antioxidant Gene Expression in HMEC-1 Cells After MeHg Treatment. HMEC-1 cells treated for 4 hours with 0.1, 1.0, and 2.0 μM MeHg in HBSS. RNA was isolated, converted to cDNA and probed for GCLC(a) and NQO1(b) using SYBRgreen qRT-PCR reagents via Applied Biosystems QuantStudio 3. Data calculated against GAPDH as a housekeeping gene. All data represent mean ± SEM. (n=3)

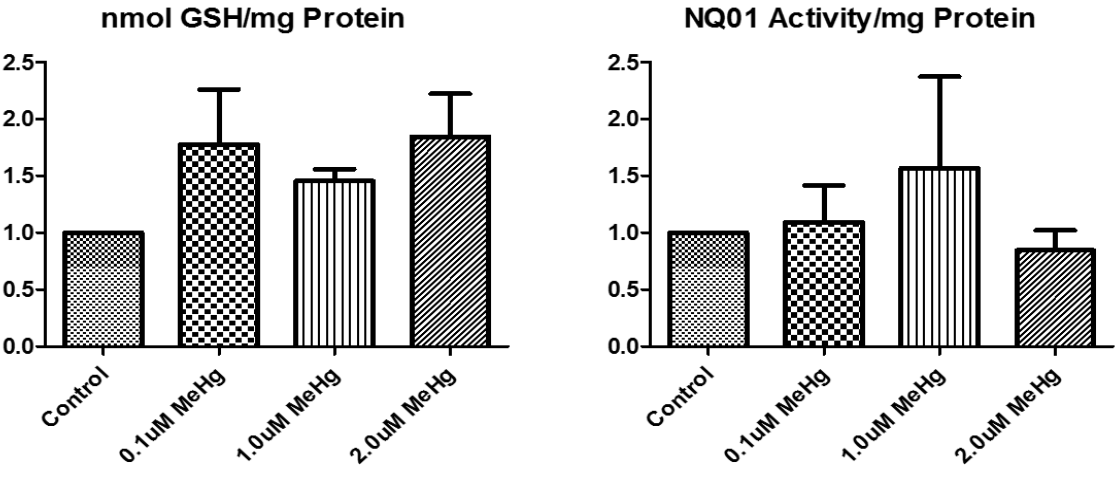

Figure 5. Phase II Antioxidant Levels in EaHy926 Cells After MeHg Treatment. (a) EAhy926 cells treated for 24 hours with 0.1, 1.0, and 2.0 μM MeHg in HBSS for 24h. GSH was calculated as a ratio of GSH to total protein. (b) EAhy926 cells treated for 24 hours with 0.1, 1.0, and 2.0 μM MeHg for 24h. NQO1 was calculated using the rate of NADPH Consumption. Samples examined using DU-800 spectrophotometer. All data represent mean ± SEM.

Methyl Mercury Effect on Cell Viability in HMEC-1 Cells

Cell viability of HMEC-1 cells was determined using flow cytometric analysis. Cells were fluorescently co-stained with FITC-labelled annexin V and propidium iodide (PI) as markers of apoptosis and necrosis, respectively. This procedure is provided in the "Materials and Methods" chapter. HMEC-1 cells treated for 4 hours with 0-2.0 μM MeHg were dyed with 7-AAD and Annexin V/PI and examined via Guava EasyCyte. No significant cytotoxicity was observed at 1 μM MeHg (**Fig. 6A-D**). However, MeHg at 2.0 μM showed a significant ($P < 0.05$) decrease in cell viability when compared to control (**Fig. 6A**). As shown in Figure 6 B-C, MeHg treatments at both 1.0 and 2.0 μM concentrations showed no significant changes in early or late apoptosis. However, rates of cell necrosis significantly increased in the 2.0μM treatment group (**Fig. 6D, Fig. 7**).

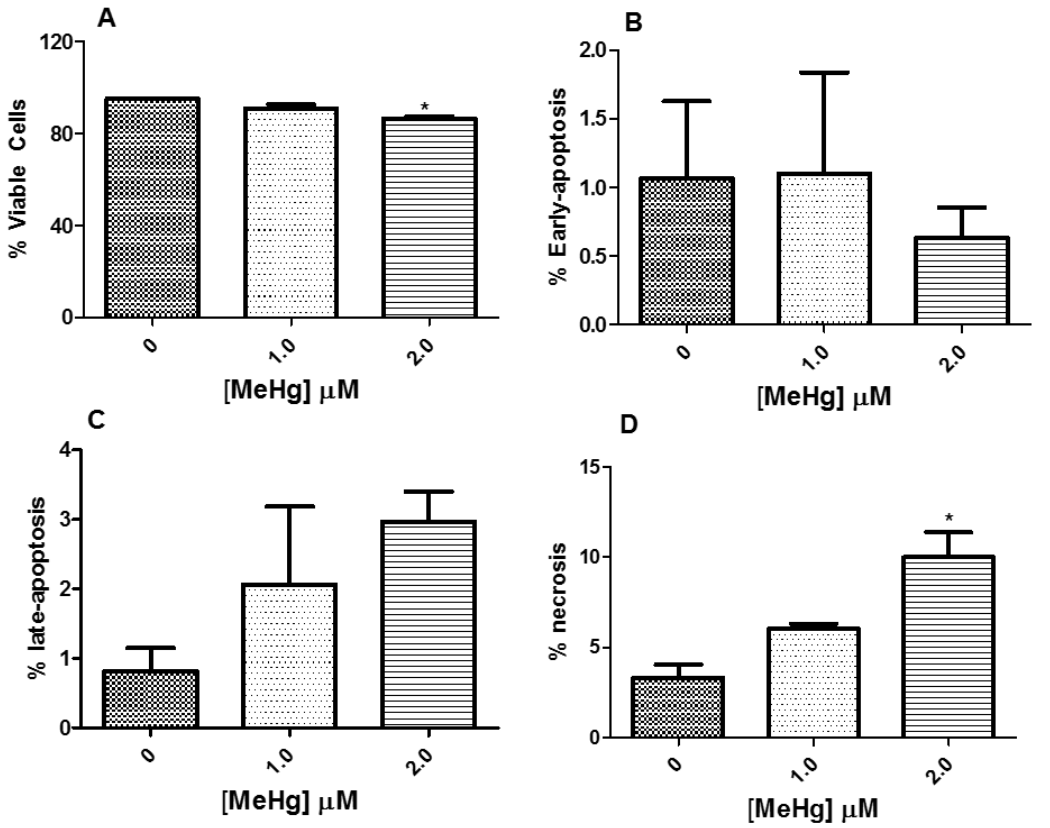

Figure 6. Flow Cytometry Results for HMEC-1 Cells Following MeHg Treatment. HMEC-1 cells were treated for 4 hours with 0.1, 1.0, and 2.0 μM MeHg in HBSS for 4 hours. 7-AAD and Annexin/PI were used as dyes to determine the difference between viable cells (A), early-apoptotic cells (B), late-apoptotic cells (C) and necrotic cells (D). Cell viability was determined using Flow Cytometric analysis via Guava EasyCyte. All data is represented as mean ± SEM. (n=3; *, $p<0.05$ vs control)

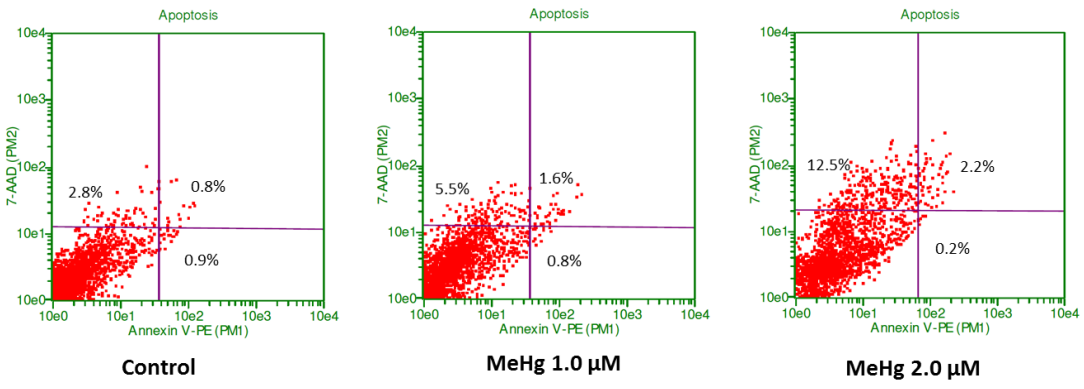

Figure 7. Representative Flow Cytometry Results in HMEC-1 Cells Following MeHg Treatment. Representative flow cytometric analysis of control HMEC-1 cells and cells exposed to MeHg at 1.0, and 2.0 µM. HMEC-1 cells were treated for 4 hours with 0.1, 1.0, and 2.0 µM MeHg in HBSS for 4 hours.

CHAPTER IV

DISCUSSION

Mercury consumption has long been implicated in a range of human health problems from behavioral disabilities to immune deficiency. More recently, greater research has been conducted into the roles of mercury on human cardiovascular health. Vascular effects of mercury consumption have been linked to oxidative stress, inflammation, thrombosis and vascular smooth muscle dysfunction. Additionally, potential clinical presentations include increased risk of hypertension, myocardial infarction, cardiac arrhythmia and carotid artery obstruction, among others [37]. Fish and seafood serve the primary source of mercury consumption for everyday human health, and studies have been conducted into the benefits versus negative health impacts of regular fish consumption. While bioaccumulation of mercury from fish consumption has been linked to CVD, Omega-3 and Omega-6 polyunsaturated fats (PUFA) present in many fish species are widely considered beneficial to the cardiovascular system and can serve to antagonize the effects of MeHg exposure [38]. Sources have suggested that vascular mercury toxicity can alter levels of intracellular antioxidants [27], promote inflammation [25], and lead to endothelial dysfunction [29]. However, further research has hypothesized that the benefits of PUFA ingestion could outweigh the negative effects of mercury ingestion [39]. These conflicting ideas only serve to underline the importance of determining the mechanism of mercury toxicity on cardiovascular health. In the

present study, we demonstrated for the first time that exposure to MeHg i*n vitro* caused a significant increase in monocyte binding in HMEC-1 cells, which would contribute to atherosclerotic development and subsequent CVD. Further, we identified increasing trends in gene expression of several inflammatory cytokines and adhesion molecules in cells treated with organic mercury as well as changes in NF-kB signaling pathway activation in macrophage-derived reporter cell lines.

Currently, the literature lacks the support that directly links MeHg exposure to monocyte adhesion and subsequent atherosclerotic development. The adhesion of circulating monocytes to vascular endothelial cells is the initiating step in the development of atherosclerosis [2-4]. Binding of these cells to an endothelial lining promotes migration into the subendothelial space followed by differentiation into macrophages, a process facilitated by contact with monocyte chemoattractant protein 1 (MCP-1/CCL2) [2-4]. These macrophages scavenge surrounding molecules before eventually becoming foam cells, which play an important role and in the early stage development of atherosclerotic lesion formation [40]. Thus, determining the extent of monocyte adhesion to endothelial cells promoted by MeHg is critical to understanding the link between organic mercury exposure and CVD. We report, for the first time, observance of an increase in monocyte adhesion following exposure to organic mercury. In our study, treatment of both 1.0 µM and 2.0 µM concentrations of MeHg yielded a significant increase in monocyte adhesion (**Fig**. **1**). This finding lends support to the hypothesis that organic mercury exposure can promote atherosclerotic development by recruitment of circulating monocytes. Our finding is consistent with a previous study by

Kim *et al.,* showing that MeHg may directly target vascular endothelial cells causing dysfunction [41]. Kim *et al.,* conducted on coronary arteries in rats exposed to MeHg have shown that even low levels of exposure induced vasoconstriction and decreased nitric oxide bioavailability. This suggests that organic mercury exposure could disrupt contraction and relaxation in heart tissue, resulting in hypertension and promoting CVD [27]. This aligns with evidence gathered linking fish consumption to elevated blood mercury levels and increased incidence of hypertension, angina, and myocardial infarction [41].

The pro-inflammatory cytokines such as IL-8 and IL-6, adhesion molecules presented on endothelial cells (ICAM-1), as well as cellular contact with MCP-1/CCL2 have been suggested to play a crucial role in regulating recruitment of monocytes to the endothelial cells [40, 42]. Levels of ICAM-1 in plasma have been linked with a pro-inflammatory response while also mediating immune cell adhesion to endothelial cells [43]. MCP-1/CCL2 is known to facilitate monocyte binding and differentiation into macrophages. This chemotactic protein binds to CCR2 receptors on migrating monocytes and induces differentiation. Studies conducted on human occlusive aortas have demonstrated that the presence of IL-8 and MCP-1 promotes immune cell recruitment and perpetuates inflammatory reactions that can lead to vessel wall destruction [44]. Another member in the interleukin chemokine family, IL-6, acts as a signaling cytokine and has been implicated in inflammation-mediated human pathologies. Studies conducted in mice not only suggest IL-6 as a marker for atherosclerosis but indicate it may contribute to atherosclerotic lesion development [45]. Further, increases in IL-6 and

ICAM-1 concentration in apparently healthy men have been linked with an increased incidence of repeat myocardial infarctions [46, 47]. Finally, studies conducted on human arterial atherosclerotic walls have found a marked increase in concentrations of both IL-6 and IL-8 [48].

The importance of the above pro-inflammatory cytokines and adhesion molecules in atherosclerotic development make them an ideal target for evaluating the links between MeHg exposure and CVD. Our results showed a significant upregulation of ICAM-1, IL-6, and MCP-1/CCL2 in the 1.0 μM and 2.0 μM MeHg treatment groups (**Fig. 2**). These results suggest that MeHg-induced monocytes binding to the endothelial cells may be partially mediated by expressions of chemokines and adhesion molecules, which further strengthen the hypothesis that MeHg exposure contributes to atherosclerosis through monocyte adhesion, migration, and differentiation in the subendothelial space. Consistent with our results in vascular endothelial cells, previous literature in other organ systems lends credence to the idea that mercury exposure can also increase these chemotactic cytokines in the different types of cells. . For example, experiments conducted on human glial cells found an increase in IL-6 production after 8 and 16-hour MeHg treatments with concentrations as low as 1.25μM [49]. Further studies performed on macrophages demonstrated increases in both IL-6 and IL-8 following treatment with varying doses of MeHg at times between 3 and 10 hours in human U937 macrophages [50]. These results in other organ systems echo our findings in endothelial cells that MeHg can contribute to the inflammatory response by upregulations of pro-inflammatory cytokines.

Previous studies have demonstrated that activation of nuclear factor-kB (NF-kB) is essential for the expression of adhesion molecules and chemokines that are critically involved in leukocyte adhesion to endothelium [51, 52]. Molecular targets of identifying NF-κB activation include proinflammatory cytokines (e.g., IL-8, IL-6, IL-2, etc.), adhesion molecules (e.g., VCAM-1 and ICAM-1), some chemokines and also cell cycle regulators[53]. Changes in the activation of this pathway can strengthen the link between MeHg exposure, endothelial dysfunction, and atherosclerosis. Identification of shifts in this pathway can grant insight into MeHg pathology. To identify the potential activation of the NF-kB pathway, we utilized the eLUCIdate™ NF-kB reporter macrophages that are designed to luminance with the addition of coelenterazine as a substrate in the event of NF-kB activation. Our results demonstrated a significant increase in the 2.0 μM MeHg treatment group suggesting that the involvement of NF-kB signaling in MeHg-induced monocyte binding to endothelial cells (**Fig. 3**). Activation of the NF-kB signaling pathway begins by decoupling and degrading the regulatory subunits, IkBα, of the NF-kB promotor, which allows translocation of the p50/p65 subunit to the nucleus to activate the pathway [54]. Thus, to further determine whether mercury-induced monocyte binding acts through activation of the NF-kB signaling pathway, future studies must be conducted to examine NF-kB regulatory subunit nuclear translocation by detection of phosphorylation of IkBα using Western Blot analysis.

Reactive oxygen species (ROS) have been identified as another contributor to monocyte adhesion in endothelium and atherosclerotic development. While ROS in normal physiological concentrations serves as signaling molecules, an overabundance of

these compounds can trigger endothelial damage, promote the production of adhesion molecules and inflammatory cytokines, and induce cell death in oversaturated foam-cell macrophages [14]. This is done by oxidation of circulating low-density lipoproteins which themselves can stimulate expression of ICAM-1, initiating the previously mentioned cascade of monocyte binding, differentiation, and terminal foam-cell apoptosis [55]. Normal regulation of these intracellular ROS is handled by phase II antioxidant enzymes such as glutathione (GSH). Analysis of the ratio between oxidized glutathione (GSSG) to its reduced form of GSH is indicative of oxidative damage, and decreases in intracellular GSH levels can suggest increased ROS generation [5]. Additionally, the enzyme NADP(H) dehydrogenase [quinone]-1 (NQO1) is a player in intracellular ROS regulation. Studies conducted propose that upregulation of NQO1 production serves as an adaptive response to intracellular oxidative stress by performing the two-electron reduction of quinones and scavenging superoxide radicals [56]. Research has provided support to the idea that MeHg exposure alters levels of these enzymes are contributing to ROS-mediated cellular dysfunction. Evaluation of Wistar rats dosed for 100 days with low levels of MeHg found a significant decrease in GSH antioxidants in blood plasma [57]. Further studies have corroborated this evidence in the nervous system as well as provided evidence of MeHg-induced ROS generation in the cardiovascular system [58, 59]. Our results conducted on EAhy 926 cardiac endothelial cells and HMEC-1 endothelial cells showed no significant changes in GSH or NQO1 in the expression of these gene markers by MeHg exposure (**Fig**. **4-5**). Longer treatment time would be needed to clarify this effect. However a reasonable explanation for the

different activation patterns in antioxidant responses to MeHg can be found in literature and pertains to the activation of the Nuclear factor-erythroid 2- related factor (Nrf2) signaling pathway [57-59] . Nrf2 induces genes which code for ROS detoxification molecules like GSH and NQO1 which are typically present following MeHg toxicity [60, 61]. Although activation of this pathway by MeHg is not fully understood, it has been demonstrated that Nrf2 binds to KEAP-1 molecules, which contain several cysteine residues. MeHg is able to bind to these residues covalently which may promote the signaling pathway. Experimental results have shown that neuroblastoma cells with elevated levels of Nrf2 expression have an increased resistance to MeHg toxicity when compared to those with standard levels of expression [61]. Interestingly, literature also exists that suggests the p65 transcription factor of the NF-kB pathway could negatively impact Nrf2 activation by competing for the transcriptional co-activator (CREB-binding protein)-p300 complex (CBP) [62, 63]. Conversely, studies conducted on different cell lines have yielded evidence that NF-kB and Nrf2 serve to promote each other. Experiments conducted in human acute myeloid leukemia cells displayed that NF-kB transcription factors could potentially induce transcription of Nrf2 [64]. In this context, the result of our studies showing no significant changes in ROS mediating phase II antioxidants and gene expression of these molecules in EAhy926 and HMEC-1 cells could be a result of aforementioned confounding signals between the NF-kB activation by MeHg (**Fig. 3**) and the possible Nrf2 signaling pathways. Therefore, future work to dissect this relationship could utilize siRNA to blow Nrf2 expression, or *in vivo* studies could employ the use of Nrf2-knockout animals. As the crosstalk between these two

pathways is complex and cell-specific, it is possible that NF-kB activation by MeHg in endothelial cells could confound downstream expression mediated by the Nrf2/Keap1 pathway of phase II antioxidant regulation. Previous studies have lent credence to the fact that necrosis versus apoptotic cell death can contribute to chemotactic and inflammatory cytokine release into the intracellular matrix, thus perpetuating atherosclerotic development[1]. Apoptotic death is an important process by which unwanted cells activate self-detrimental pathways to induce death to maintain constant size and regulate cell production [65-67]. Necrosis, on the other hand, appears to be invoked by extrinsic sources causing acute cellular dysfunction. Recent studies using TEM analysis of human atherosclerotic lesions have shown that a great deal of cell death in these tissues is due to necrosis [67-69]. Thus, it would be beneficial to determine the type of cell death occurring as a result of MeHg exposure, as necrotic cell death could further bolster the induced inflammatory response. Our studies using flow cytometric analysis of HMEC-1 cells with 7-AAD and Annexin V/PI showed a significant decrease in cell viability at 2.0 μM concentrations, specifically, a significant increase in necrotic cell populations without invoking apoptosis (**Fig**. **6**). This indicates that high concentrations of MeHg can cause severe damage to cellular membranes, increasing the presence of the aforementioned inflammatory cytokines and chemotactic molecules, contributing to atherosclerosis. However, 1.0 μM concentrations of MeHg showed no significant changes in cell death type despite upregulating expression of the same chemotactic and inflammatory markers. Future experiments must be performed to explore whether MeHg

induced necrosis was significantly contributing to atherosclerotic development both *in vitro* and *in vivo*.

It would be pertinent to note that blood concentrations of Hg (chiefly MeHg), have been reported up to ~1μM (~200 ng Hg/ml) in human subjects following accidental exposure to MeHg, and only decreased to ~0.13 μM after 3 months of clearance [70]. A study conducted identifying the concentrations of mercury found in fish samples destined for human consumption by X-ray absorption found levels as low as 0.4 μM and as high as 6.0 μM [71]. However, this mercury was found in various forms including conformations already bound to thiol groups. Further consideration must be taken to factor in the bioaccumulation of mercury in physiological systems. With a half-life of ~70 days, it's possible for mercury levels to increase steadily with repeated consumption of mercury-contaminated foods [72]. Additional factors involved in our decision to use these concentrations include other studies conducted *in vitro* spanning concentrations of 0.1 μM to 20 μM [73]. With this knowledge, MeHg concentrations from 0.1 μM to ~1.0μM were used in this study, which we considered to be acutely non-lethal, physiologically relevant, and certainly achievable *in vivo [70]*.

To summarize this study, we demonstrated for the first time that *in vitro* MeHg exposure to HMEC-1 cells causes a significant increase in monocyte binding, a quality that would contribute to atherosclerotic development and subsequent CVD. A significant increase in the expression of inflammatory and chemotactic cytokines including ICAM-1, IL-6, IL-8, and MCP-1/CCL2 was also observed, which would contribute to monocyte adhesion and binding. Additionally, observation of the activation of NF-kB suggests that

MeHg-induced adhesion of monocytes to endothelial cells is associated with this pathway, which can further facilitate the production of cytokines and adhesion molecules. This study provides new insight into the molecular actions of MeHg that can lead to endothelial injury, inflammation, and subsequent atherosclerosis. This data will contribute to our understanding of the detrimental effects involved in MeHg on human health, especially as this exposure exacerbates with the spread of global industrialization.

REFERENCES

1. Stoneman, V.E. and M.R. Bennett, *Role of apoptosis in atherosclerosis and its therapeutic implications.* Clin Sci (Lond), 2004. **107**(4): p. 343-54.
2. Mestas, J. and K. Ley, *Monocyte-endothelial cell interactions in the development of atherosclerosis.* Trends Cardiovasc Med, 2008. **18**(6): p. 228-32.
3. Marui, N., et al., *Vascular cell adhesion molecule-1 (VCAM-1) gene transcription and expression are regulated through an antioxidant-sensitive mechanism in human vascular endothelial cells.* J Clin Invest, 1993. **92**(4): p. 1866-74.
4. Solovjov, D.A., E. Pluskota, and E.F. Plow, *Distinct roles for the alpha and beta subunits in the functions of integrin alphaMbeta2.* J Biol Chem, 2005. **280**(2): p. 1336-45.
5. Tavakoli, S. and R. Asmis, *Reactive oxygen species and thiol redox signaling in the macrophage biology of atherosclerosis.* Antioxid Redox Signal, 2012. **17**(12): p. 1785-95.
6. Gilmore, T.D., *Introduction to NF-kappaB: players, pathways, perspectives.* Oncogene, 2006. **25**(51): p. 6680-4.
7. Griendling, K.K., D. Sorescu, and M. Ushio-Fukai, *NAD (P) H oxidase: role in cardiovascular biology and disease.* Circulation research, 2000. **86**(5): p. 494-501.
8. Madamanchi, N.R., A. Vendrov, and M.S. Runge, *Oxidative stress and vascular disease.* Arterioscler Thromb Vasc Biol, 2005. **25**(1): p. 29-38.
9. Cominacini, L., et al., *Oxidized low density lipoprotein (ox-LDL) binding to ox-LDL receptor-1 in endothelial cells induces the activation of NF-kappaB through an increased production of intracellular reactive oxygen species.* J Biol Chem, 2000. **275**(17): p. 12633-8.
10. Kattoor, A.J., et al., *Oxidative Stress in Atherosclerosis.* Curr Atheroscler Rep, 2017. **19**(11): p. 42.
11. Hulsmans, M., E. Van Dooren, and P. Holvoet, *Mitochondrial reactive oxygen species and risk of atherosclerosis.* Curr Atheroscler Rep, 2012. **14**(3): p. 264-76.
12. Schneider, C., et al., *Two distinct pathways of formation of 4-hydroxynonenal. Mechanisms of nonenzymatic transformation of the 9- and 13-hydroperoxides of linoleic acid to 4-hydroxyalkenals.* J Biol Chem, 2001. **276**(24): p. 20831-8.
13. Valko, M., et al., *Free radicals and antioxidants in normal physiological functions and human disease.* Int J Biochem Cell Biol, 2007. **39**(1): p. 44-84.
14. Cai, H. and D.G. Harrison, *Endothelial dysfunction in cardiovascular diseases: the role of oxidant stress.* Circ Res, 2000. **87**(10): p. 840-4.
15. Pastinszky, I., *[Pigmentation disorders of the face in internal diseases]*. Orv Hetil, 1973. **114**(3): p. 150-2.

16. Rice, K.M., et al., *Environmental mercury and its toxic effects.* J Prev Med Public Health, 2014. **47**(2): p. 74-83.
17. Ikem, A. and N.O. Egiebor, *Assessment of trace elements in canned fishes (mackerel, tuna, salmon, sardines and herrings) marketed in Georgia and Alabama (United States of America).* Journal of food composition and analysis, 2005. **18**(8): p. 771-787.
18. Harada, M., *Minamata disease: methylmercury poisoning in Japan caused by environmental pollution.* Critical reviews in toxicology, 1995. **25**(1): p. 1-24.
19. Farina, M., M. Aschner, and J.B. Rocha, *Oxidative stress in MeHg-induced neurotoxicity.* Toxicology and applied pharmacology, 2011. **256**(3): p. 405-417.
20. da Silva Santana, L.N., et al., *Low doses of methylmercury exposure during adulthood in rats display oxidative stress, neurodegeneration in the motor cortex and lead to impairment of motor skills.* Journal of Trace Elements in Medicine and Biology, 2019. **51**: p. 19-27.
21. Grandjean, P., et al., *Cognitive deficit in 7-year-old children with prenatal exposure to methylmercury.* Neurotoxicology and teratology, 1997. **19**(6): p. 417-428.
22. Grotto, D., et al., *Mercury exposure and oxidative stress in communities of the Brazilian Amazon.* Science of the total environment, 2010. **408**(4): p. 806-811.
23. Larsen, T.J., et al., *Whole blood mercury and the risk of cardiovascular disease among the Greenlandic population.* Environmental research, 2018. **164**: p. 310-315.
24. Zhang, Y., et al., *Associations between total mercury and methyl mercury exposure and cardiovascular risk factors in us adolescents.* Environmental Science and Pollution Research, 2018. **25**(7): p. 6265-6272.
25. Salonen, J.T., et al., *Intake of mercury from fish, lipid peroxidation, and the risk of myocardial infarction and coronary, cardiovascular, and any death in eastern Finnish men.* Circulation, 1995. **91**(3): p. 645-655.
26. Marques, R.C., et al., *Maternal mercury exposure and neuro-motor development in breastfed infants from Porto Velho (Amazon), Brazil.* international Journal of Hygiene and environmental Health, 2007. **210**(1): p. 51-60.
27. Furieri, L.B., et al., *Endothelial dysfunction of rat coronary arteries after exposure to low concentrations of mercury is dependent on reactive oxygen species.* British journal of pharmacology, 2011. **162**(8): p. 1819-1831.
28. Nishikawa, Y. and S. Ogawa, *Importance of nitric oxide in the coronary artery at rest and during pacing in humans.* Journal of the American College of Cardiology, 1997. **29**(1): p. 85-92.
29. Wiggers, G.A., et al., *Low mercury concentrations cause oxidative stress and endothelial dysfunction in conductance and resistance arteries.* American Journal of Physiology-Heart and Circulatory Physiology, 2008.
30. Lund, B.-O., D.M. Miller, and J.S. Woods, *Studies on Hg (II)-induced H2O2 formation and oxidative stress in vivo and in vitro in rat kidney mitochondria.* Biochemical pharmacology, 1993. **45**(10): p. 2017-2024.

31. Mayer, K., et al., *Omega-3 fatty acids suppress monocyte adhesion to human endothelial cells: role of endothelial PAF generation.* Am J Physiol Heart Circ Physiol, 2002. **283**(2): p. H811-8.
32. Chen, J.W., et al., *Ginkgo biloba extract inhibits tumor necrosis factor-alpha-induced reactive oxygen species generation, transcription factor activation, and cell adhesion molecule expression in human aortic endothelial cells.* Arterioscler Thromb Vasc Biol, 2003. **23**(9): p. 1559-66.
33. Carluccio, M.A., et al., *Olive oil and red wine antioxidant polyphenols inhibit endothelial activation: antiatherogenic properties of Mediterranean diet phytochemicals.* Arterioscler Thromb Vasc Biol, 2003. **23**(4): p. 622-9.
34. Read, M.A., et al., *NF-kappa B and I kappa B alpha: an inducible regulatory system in endothelial activation.* J Exp Med, 1994. **179**(2): p. 503-12.
35. Brown, K., et al., *Control of I kappa B-alpha proteolysis by site-specific, signal-induced phosphorylation.* Science, 1995. **267**(5203): p. 1485-8.
36. Ouchi, N., et al., *Adiponectin, an adipocyte-derived plasma protein, inhibits endothelial NF-kappaB signaling through a cAMP-dependent pathway.* Circulation, 2000. **102**(11): p. 1296-301.
37. Houston, M., *The Role of Mercury in Cardiovascular Disease.* Journal of Cardiovascular Diseases and Diagnosis, 2014. **2**(5).
38. Houston, M.C., *Role of mercury toxicity in hypertension, cardiovascular disease, and stroke.* J Clin Hypertens (Greenwich), 2011. **13**(8): p. 621-7.
39. Mozaffarian, D. and E.B. Rimm, *Fish intake, contaminants, and human health: evaluating the risks and the benefits.* JAMA, 2006. **296**(15): p. 1885-99.
40. Libby, P., *Inflammation in atherosclerosis.* Nature, 2002. **420**(6917): p. 868-74.
41. Kim, Y.N., et al., *Relationship between Blood Mercury Level and Risk of Cardiovascular Diseases: Results from the Fourth Korea National Health and Nutrition Examination Survey (KNHANES IV) 2008-2009.* Prev Nutr Food Sci, 2014. **19**(4): p. 333-42.
42. Boisvert, W.A., et al., *A leukocyte homologue of the IL-8 receptor CXCR-2 mediates the accumulation of macrophages in atherosclerotic lesions of LDL receptor-deficient mice.* J Clin Invest, 1998. **101**(2): p. 353-63.
43. Lawson, C. and S. Wolf, *ICAM-1 signaling in endothelial cells.* Pharmacol Rep, 2009. **61**(1): p. 22-32.
44. Koch, A.E., et al., *Enhanced production of the chemotactic cytokines interleukin-8 and monocyte chemoattractant protein-1 in human abdominal aortic aneurysms.* Am J Pathol, 1993. **142**(5): p. 1423-31.
45. Huber, S.A., et al., *Interleukin-6 exacerbates early atherosclerosis in mice.* Arterioscler Thromb Vasc Biol, 1999. **19**(10): p. 2364-7.
46. Ridker, P.M., et al., *Plasma concentration of interleukin-6 and the risk of future myocardial infarction among apparently healthy men.* Circulation, 2000. **101**(15): p. 1767-72.
47. Ridker, P.M., et al., *Plasma concentration of soluble intercellular adhesion molecule 1 and risks of future myocardial infarction in apparently healthy men.* Lancet, 1998. **351**(9096): p. 88-92.

48. Rus, H.G., R. Vlaicu, and F. Niculescu, *Interleukin-6 and interleukin-8 protein and gene expression in human arterial atherosclerotic wall.* Atherosclerosis, 1996. **127**(2): p. 263-71.
49. Chang, J.Y., *Methylmercury causes glial IL-6 release.* Neurosci Lett, 2007. **416**(3): p. 217-20.
50. Yamamoto, M., et al., *Activation of interleukin-6 and -8 expressions by methylmercury in human U937 macrophages involves RelA and p50.* J Appl Toxicol, 2017. **37**(5): p. 611-620.
51. Boyle, E.M., Jr., et al., *Inhibition of nuclear factor-kappa B nuclear localization reduces human E-selectin expression and the systemic inflammatory response.* Circulation, 1998. **98**(19 Suppl): p. II282-8.
52. Nallasamy, P., et al., *Sulforaphane reduces vascular inflammation in mice and prevents TNF-alpha-induced monocyte adhesion to primary endothelial cells through interfering with the NF-kappaB pathway.* J Nutr Biochem, 2014. **25**(8): p. 824-33.
53. Liu, T., et al., *NF-κB signaling in inflammation.* Signal transduction and targeted therapy, 2017. **2**: p. 17023.
54. Morgan, M.J. and Z.G. Liu, *Crosstalk of reactive oxygen species and NF-kappaB signaling.* Cell Res, 2011. **21**(1): p. 103-15.
55. Kita, T., et al., *Role of oxidized LDL in atherosclerosis.* Ann N Y Acad Sci, 2001. **947**: p. 199-205; discussion 205-6.
56. Li, L., et al., *Nrf2/ARE pathway activation, HO-1 and NQO1 induction by polychlorinated biphenyl quinone is associated with reactive oxygen species and PI3K/AKT signaling.* Chem Biol Interact, 2014. **209**: p. 56-67.
57. Grotto, D., et al., *Low level and sub-chronic exposure to methylmercury induces hypertension in rats: nitric oxide depletion and oxidative damage as possible mechanisms.* Arch Toxicol, 2009. **83**(7): p. 653-62.
58. Kaur, P., M. Aschner, and T. Syversen, *Glutathione modulation influences methyl mercury induced neurotoxicity in primary cell cultures of neurons and astrocytes.* Neurotoxicology, 2006. **27**(4): p. 492-500.
59. Lemos, N.B., et al., *Low mercury concentration produces vasoconstriction, decreases nitric oxide bioavailability and increases oxidative stress in rat conductance artery.* PLoS One, 2012. **7**(11): p. e49005.
60. Kensler, T.W., N. Wakabayashi, and S. Biswal, *Cell survival responses to environmental stresses via the Keap1-Nrf2-ARE pathway.* Annu Rev Pharmacol Toxicol, 2007. **47**: p. 89-116.
61. Hwang, G.W., *Role of intracellular defense factors against methylmercury toxicity.* Biol Pharm Bull, 2012. **35**(11): p. 1881-4.
62. Yu, M., et al., *Nuclear factor p65 interacts with Keap1 to repress the Nrf2-ARE pathway.* Cell Signal, 2011. **23**(5): p. 883-92.
63. Wardyn, J.D., A.H. Ponsford, and C.M. Sanderson, *Dissecting molecular cross-talk between Nrf2 and NF-kappaB response pathways.* Biochem Soc Trans, 2015. **43**(4): p. 621-6.

64. Rushworth, S.A., et al., *The high Nrf2 expression in human acute myeloid leukemia is driven by NF-kappaB and underlies its chemo-resistance.* Blood, 2012. **120**(26): p. 5188-98.
65. Nicholson, D.W. and N.A. Thornberry, *Apoptosis. Life and death decisions.* Science, 2003. **299**(5604): p. 214-5.
66. Thompson, C.B., *Apoptosis in the pathogenesis and treatment of disease.* Science, 1995. **267**(5203): p. 1456-62.
67. Jia, Z. and H.P. Misra, *Exposure to mixtures of endosulfan and zineb induces apoptotic and necrotic cell death in SH-SY5Y neuroblastoma cells, in vitro.* J Appl Toxicol, 2007. **27**(5): p. 434-46.
68. Martinet, W., D.M. Schrijvers, and G.R. De Meyer, *Necrotic cell death in atherosclerosis.* Basic Res Cardiol, 2011. **106**(5): p. 749-60.
69. Gu, Z., et al., *S-nitrosylation of matrix metalloproteinases: signaling pathway to neuronal cell death.* Science, 2002. **297**(5584): p. 1186-90.
70. Gupta, M., J.K. Bansal, and C.M. Khanna, *Blood mercury in workers exposed to the preparation of mercury cadmium telluride layers on cadmium telluride base.* Ind Health, 1996. **34**(4): p. 421-5.
71. Harris, H.H., I.J. Pickering, and G.N. George, *The chemical form of mercury in fish.* Science, 2003. **301**(5637): p. 1203.
72. Clarkson, T.W., L. Magos, and G.J. Myers, *The toxicology of mercury--current exposures and clinical manifestations.* N Engl J Med, 2003. **349**(18): p. 1731-7.
73. Antunes Dos Santos, A., et al., *Methylmercury and brain development: A review of recent literature.* J Trace Elem Med Biol, 2016. **38**: p. 99-107.